Supramolecular Chemistry
Publication details, including instructions for authors and subscription information:
http://www.informaworld.com/smpp/title~content=t713649759

Assembled Columnar Structures from bis-urea Macrocycles

Linda S. Shimizu[a]; Andrew D. Hughes[a]; Mark D. Smith[a]; Stevan A. Samuel[a]; Delia Ciurtin-Smith[a]
[a] Department of Chemistry and Biochemistry, University of South Carolina, Columbia, SC, USA

To cite this Article Shimizu, Linda S. , Hughes, Andrew D. , Smith, Mark D. , Samuel, Stevan A. and Ciurtin-Smith, Delia(2005) 'Assembled Columnar Structures from bis-urea Macrocycles', Supramolecular Chemistry, 17: 1, 27 — 30
To link to this Article: DOI: 10.1080/10610270412331328989
URL: http://dx.doi.org/10.1080/10610270412331328989

Supramolecular Chemistry, January–March 2005 Vol. 17 (1–2), pp. 27–30

Taylor & Francis
Taylor & Francis Group

Assembled Columnar Structures from bis-urea Macrocycles

LINDA S. SHIMIZU*, ANDREW D. HUGHES, MARK D. SMITH, STEVAN A. SAMUEL and DELIA CIURTIN-SMITH

Department of Chemistry and Biochemistry, University of South Carolina, Columbia, SC 29208, USA

Received (in Austin, USA) 24 July 2004; Accepted 19 September 2004

Presented is a review of our research on using macrocyclic bis-ureas as supramolecular building blocks. These macrocycles predictably self-assemble into columnar structures via strong urea–urea hydrogen bonds and pi–stacking interactions. We developed a facile synthetic route to these macrocyclic ureas, confirmed their self-assembly pattern, and are now assessing their potential as a supramolecular building block. A series of bis-urea macrocycles were synthesized and assembled to verify the fidelity of their self-assembly motifs. Ultimately, a large phenylether bis-urea macrocycle was synthesized that formed tubular assemblies containing a guest accessible channel. We have characterized the structure of the assembled nanotubes by NMR and X-ray crystallography and evaluated this new porous solid with respect to its binding properties and specificity. This porous self-assembled material is thermally and chemically stable and can reversibly bind and exchange a variety of guest molecules.

Keywords: Ureas; Self-assembly; Nanotubes; Crystal structures

Designer porous materials are of great interest due to potential applications in biology, chemistry and material science. One method of constructing porous nanotubular structures is from the self-assembly of rigid macrocycles. Self-assembly of macrocycles favors the formation of cavities of predetermined dimensions and inhibits interpenetrated structures, which might otherwise obstruct the desired cavities. This strategy has been successfully applied by a number of groups using a variety of cyclic building blocks, such as cyclic peptides and macrocyclic polyphenyleneethylenes, to name just a few [1–3]. We have investigated the use of symmetrical macrocyclic bis-ureas [4,5]. The ureas form strong 3-centered intermolecular hydrogen bonds [6] and drive the self-assembly of the macrocyles directly on top of each other to form columns (Figures 1 and 2). The larger bis-urea macrocycles, upon tubular self-assembly, contain a channel that can reversibly bind a variety of different guest molecules.

The symmetrical bis-ureas were modularly constructed from rigid spacers and ureas. Rigid aryl spacers prevent collapse of the cavity and preorganize the ureas perpendicular to the plane of the macrocycle, which is an ideal orientation for intermolecular hydrogen bond formation. We were able to successfully develop the synthesis of the desired bis-ureas, allowing rapid construction, purification and quantitative deprotection of bis-urea macrocycles. Key to the synthesis was the introduction of the ureas as protected cyclic triazones, which prevented over alkylation as well as inhibited premature aggregation [7,8].

Bis-urea macrocycles **1**–**3** have been synthesized and characterized by NMR and X-Ray crystallography. The smallest bis-urea macrocycles were synthesized first. The macrocycles were formed using simple, rigid *meta*- and *para*-xylene spacers. Although they are too small to have any internal cavity they offered confirmation of the predicted urea–urea hydrogen bonding interactions and also suggested ideal geometries for the second generation of macrocycle components. The design of this first generation of bis-urea macrocycles were evaluated by molecular modeling using MacroModel [9] prior to synthesis, which indicated that the bent *m*-xylene spacer in bis-urea **1** would be better in presenting the bis-ureas in the desired orientation than the more linear *p*-xylene spacer which formed a strained macrocyclic structure **2**. Synthesis of the bis-ureas proceeded from triazone 4 and the corresponding dibromide. For example, reaction of *t*-butyl triazone **4** with *p*-dibromoxylene afforded the protected

*Corresponding author. E-mail: shimizul@mail.chem.sc.edu

ISSN 1061-0278 print/ISSN 1029-0478 online © 2005 Taylor & Francis Ltd
DOI: 10.1080/10610270412331328989

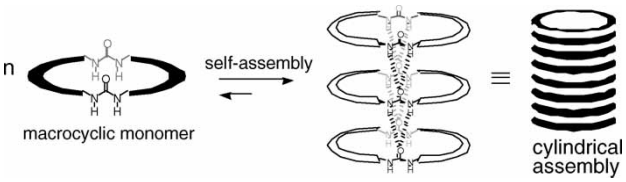

FIGURE 1 Schematic representation of the self-assembly of bis-ureas macrocycles into a nanotube.

bis-urea macrocycle **5** (Scheme 1). Deprotection was accomplished in high yields with diethanol amine in methanol to give bis-urea macrocycle **2**.

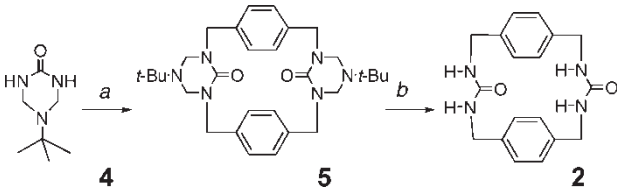

SCHEME 1 [a]*Reagents and conditions:* (a) NaH, THF, *para*-α,α′-dibromoxylylene, 10%. (b) 20% diethanolamine, MeOH, reflux, 90%.

EXPERIMENTAL

Crystal Structures

Structures for compounds **1** (CCDC reference number 116911) and **3** (CCDC reference number 228322) have been reported previously [4,5].

Synthesis of *p*-xylene Macrocycle 2

Prepared in two steps from tert-butyl triazone and *para*-α,α′-dibromoxylylene. ^{1}H NMR (400 MHz, DMSO) δ ppm = 6.97 (s, 8H), 6.28 (t, 4H, J = 6.7 Hz), 3.96 (br s, 8H). ^{13}C NMR (133 MHz, DMSO) δ ppm = 159.5, 139.5, 127.1, 43.4. The *p*-xylene macrocycle **2**, formed clear colorless crystals from DMSO.

Crystallographic Data

For **2** (CCDC reference number 244496). The *p*-xylene macrocycle **2**, $C_{18}H_{20}N_4O_4{\cdot}2H_2O$, M = 360.11, monoclinic, space group P 21/c, $a = 10.1143(15)$ Å, $b = 5.1287(8)$ Å, $c = 16.495(2)$ Å, $\alpha = 90°$. $\beta = 93.435(3)°$. $\gamma = 90°$. $U = 854.1$ Å^3, $Z = 2$, $D_c = 1.401$ Mg m^{-3}, $\lambda = 0.71073$ Å, (Mo-Kα), F(000) = 344, Bruker SMART APEX CCD-based diffractometer system, crystal size $0.66 \times 0.07 \times 0.03$ mm^3, $\alpha = 0.101$ mm^{-1}, reflections collected = 4717, independent reflections = 1746, R(int) = 0.0633, R1 = 0.0423, wR2 = 0.0821.

Guest desorption studies were conducted on a TA Instruments SDT-2960 simultaneous DTA-TGA at a heating rate of 1°C/min from 30 to 150°C under Helium. TGA experiments were carried out on 5–10 mg of sample. Upon completion, the sample was recollected for the next adsorption–desorption study.

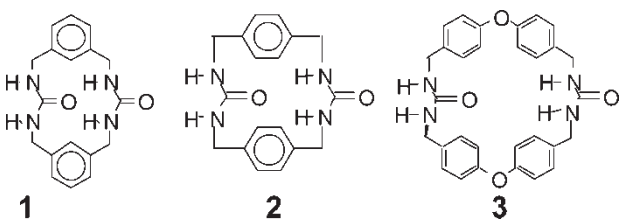

FIGURE 2 Bis-urea macrocycles synthesized and characterized by X-ray crystallography.

DISCUSSION

The urea groups provide strong interactions that drive the assembly even in polar solvents. Single crystals of the *meta*-xylene bis-urea **1** assembled from refluxing glacial acetic acid, and the strained *para*-xylene **2** gave single crystals from DMSO. The crystal structure of **1** reveals the expected columnar assembly with the urea carbonyls aligned in opposite directions, minimizing dipole interactions (Figure 3). The extended structure shows that the individual bis-urea units stacked on top of each other to form a supramolecular tubular structure. The bis-urea monomers are held together by three-centered head to tail urea hydrogen bonding motif extending along both sides of the tube and by aryl stacking interactions.

The *para*-substituted analog **2** also assembled into columnar structures (Figure 4); however ring strain appears to be an important consideration in the synthesis and assembly of the bis-ureas, as it makes ring closure more difficult (10% versus 20% yield for the cyclization steps for the para and

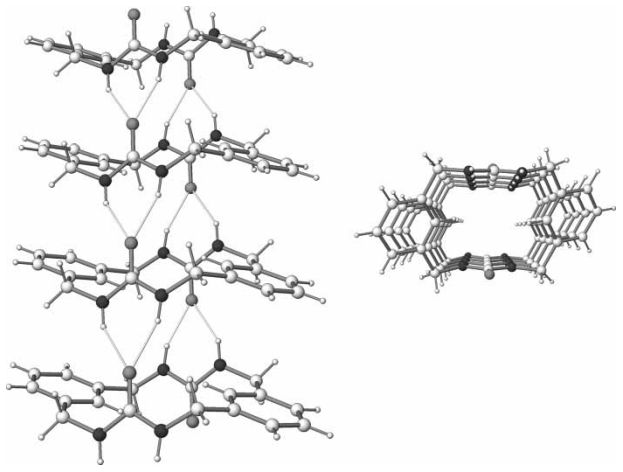

FIGURE 3 X-ray diffraction of the bis-urea macrocycle **1**. (left) View alongside a single tube showing the urea–urea hydrogen bonding pattern. (right) View down a single tube.

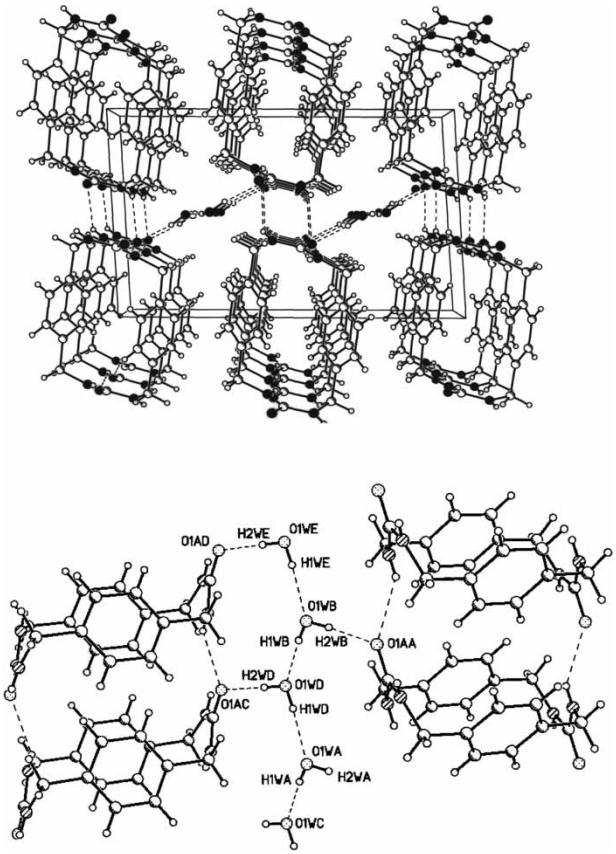

FIGURE 4 X-ray structure of *para*-xylene bis-urea **2**. (top) View down columnar structures. (bottom) Simplified view of packing showing the relationship of two adjacent tubes bridged by a channel of ordered water molecules.

meta-macrocycles, respectively) and disrupts the planarity of the urea groups. In the strained *para*-substituted analogue **4** the ureas are twisted with one NH no longer in the same plane as the urea carbonyl, yielding a much weaker amide–amide interaction. The second NH is not involved in the stacking interaction and instead forms hydrogen-bonds to intervening water molecules (Figure 4, bottom).

These studies also gave insight into important design considerations. More linear spacers are not ideal as they can give strained cycles, disrupt urea planarity, and minimize cavity size. Instead, rigid linkers should incorporate a bend angle. With this information we synthesized the larger bis-urea **3**, which by molecular modeling contained a sizeable cavity. X-ray quality crystals of **3** were obtained from superheated acetic acid, 128°C. The crystal structure of **3** revealed the desired molecular structure and extended organization (Figure 5). The extended structure showed the individual bis-urea units stacking on top of each other, forming a supra-molecular tubular structure. Individual tubes, again, exhibited three-centered head to tail urea hydrogen bonding extending along both sides of the tube as

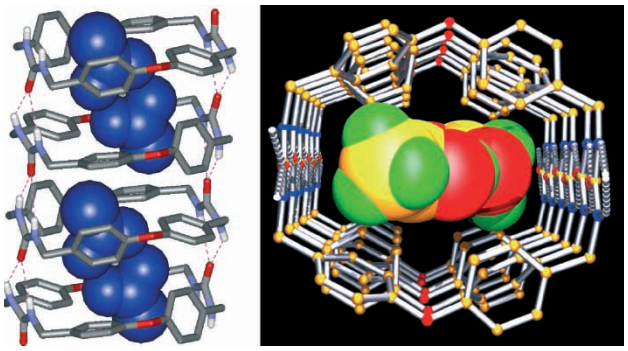

FIGURE 5 A view alongside (left) and down (right) a single tube from the X-ray structure of **3**. The guest is acetic acid.

well as aromatic stacking interactions between the phenylether spacers. As predicted, the nanotube has a sizeable rectangular central cavity, which contained well-ordered acetic acid dimers.

Crystallizations of **3**, formed thin, elongated crystals, which were generally too small for X-ray analysis; however, these small crystals have remarkable host–guest properties. We first tested the stability of assembled **3** in the absence of guest by TGA (Figure 6) and measured a repeatable weight loss of 11.61% between 30 and 90°C. This weight loss was consistent with removal of all the acetic acid guest molecules (calculated weight loss, 10.56%), corresponding to a 1:1 molar ratio of host:guest. The stoichiometry of the filled channels as well as the absence of guest following evacuation by TGA was confirmed by ^{1}H NMR by dissolving the crystals in DMSO-d_6. Most excitingly, the empty assembled **3**, remained crystalline. These crystals rebound acetic acid upon exposure to acetic acid vapor in a sealed chamber for 72 hours, exhibiting a nearly identical

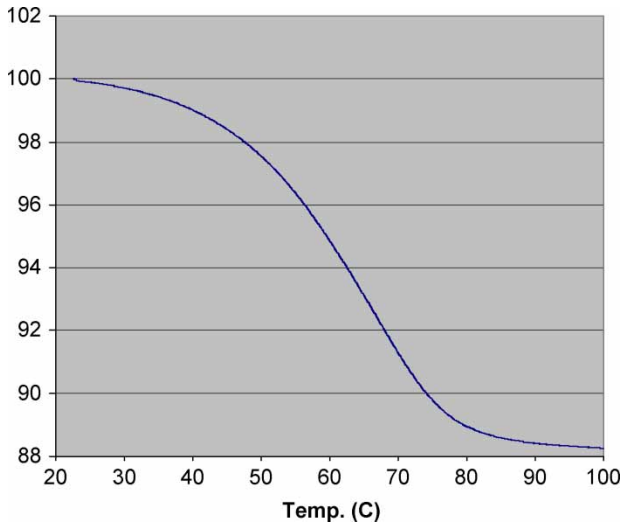

FIGURE 6 TGA of **3**(AcOH (23 to 100°C at 1 deg/min) exhibited a weight loss of 11.61% between 30 and 90°C. After exposure to acetic acid vapor, the crystals exhibited a nearly identical weight loss of 11.61% between 30 and 90°C followed by reloading of acetic acid guest.

TABLE I Guest desorption from assembled 3 measured by TGA

Guest	Observed weight loss[†]	Host:guest	Calculated weight loss	Guest vol (Å)
acetic acid	11.3%	1:1	10.6%	52
t-butanol	0%	–	–	89
ethyl acetate	7.5%	2:1	8.0%	88
DMSO	14.2%	1:1	13.3%	72
THF	6.9%	2:1	6.6%	78

[†]TGA were run for a variety of guest molecules. Averages observed weight loss was calculated for 10 runs in acetic acid and three runs for the other solvents that bound.

weight loss curve by TGA (11.02% weight loss). The same crystals rebound and released acetic acid a third time exhibiting an 11.34% weight loss by TGA. Other crystals of assembled **3**, exhibited the same binding properties and the average weight loss for 10 different TGA runs of assembled **3**·AcOH was 11.26%.

Further evidence for the structural stability of the empty nanotube assembly and the reversibility of the binding process was provided by powder X-ray diffraction (PXRD). The guest filled crystals were ground to a powder and examined by PXRD. The PXRD data was reexamined after guest removal and exhibited a slightly different PXRD but still appeared to maintain a well-defined structure. Following retreatment of the evacuated solid with acetic acid vapor a third PXRD was observed which has peak positions and intensities nearly identical to the original acetic acid bound structure.

We examined the affinity of assembled **3** for a variety of other solvents, by exposing empty assembled **3** to solvent vapor in a sealed chamber for 12 to 72 hours. Table I lists the weight loss observed by TGA for a variety of guests bound by assembled **3**. Both DMSO and acetic acid were absorbed in 1:1 stoichiometry (cycle:guest), while the larger THF and ethyl acetate were bound in 2:1 (cycle:guest) stoichiometry. Guest absorption/desorption was repeatable, giving nearly identical weight loss curves and the table lists the average observed weight loss by TGA for a minimum of three separate absortion/desorption experiments for each solvent that bound. The fact that these tubes repeatedly absorb guests with the same stoichiometry experimentally suggests that the guests are fairly ordered within the columns. Additionally, the tubes can be reused and after absorption/desorption studies with each of the new solvents in Table I, the empty tubes were able to reabsorb acetic acid again in 1:1 stoichiometry. We are currently examining the affinity, selectivity and mechanism of binding and release of assembled **3** for a wider range of guests and will report on this in due course.

In summary, we have verified our ability to synthesize these macrocyclic bis-ureas, confirmed their assembly patterns, and demonstrated that they contain a guest-accessible channel. We are embarking on the synthesis of third generation bis-urea macrocycles from expanded rigid spacers that vary the cavity size and interior properties of the macrocycle, generating "tunable" cavities, designed to bind specific guests. The modular construction of these macrocycles from rigid spacers and protected ureas should enable the large-scale synthesis of similar tubular materials and enhance their viability in practical applications.

Acknowledgements

This work was supported by the NSF (Grant No. 9973132.)

References

[1] Ghadiri, M. R.; Granja, J. R.; Milligan, R. A.; McRee, D. E.; Khazanovich, N. *Nature* **1993**, *366*, 324.
[2] Olenyuk, B.; Stang, R. J. *Acc. Chem. Res.* **1997**, *30*, 502.
[3] Shetty, A. S.; Zhang, J. S.; Moore, J. S. *J. Am. Chem. Soc.* **1988**, *118*, 1019.
[4] Shimizu, L. S.; Smith, M. D.; Hughes, A. D.; Shimizu, K. D. *Chem. Commun.* **2001**, 1592.
[5] Shimizu, L. S.; Hughes, A. D.; Smith, M. D.; Davis, M. J.; Zhang, P.; zur Loye, H.-C.; Shimizu, K. D. *J. Am. Chem. Soc.* **2003**, *125*, 14972.
[6] Etter, M. C.; Urbanczyk-Lipkowska, X.; Zia-Ebrahimi, M.; Panuto, T. W. *J. Am. Chem. Soc.* **1990**, *112*, 8415.
[7] Petersen, H. *Synthesis* **1973**, 243.
[8] Knapp, S.; Hale, J. J.; Bastos, M.; Gibson, F. S. Amino protection using triazones *Tet. Letters* **1990**, *31*, 2109.
[9] Macromodel version 5.5, Columbia University, Silicon Graphics Inc.